

APPLICATION OF NUMERICAL INTEGRATION IN ANALYSING THE VOLUME OF REINFORCEMENT PARTICLES IN ALGORITHMS FOR GENERATING REPRESENTATIVE VOLUME ELEMENTS (RVEs)

Grzegorz MIECZKOWSKI*, Dariusz SZPICA*, Andrzej BORAWSKI*

*Faculty of Mechanical Engineering, Białystok University of Technology, ul. Wiejska 45C, 15-351 Białystok, Poland

g.mieczkowski@pb.edu.pl, d.szpica@pb.edu.pl, a.borawski@pb.edu.pl

received 13 November 2023, revised 16 May 2024, accepted 20 May 2024

Abstract: The paper focuses on spatial modelling of composites with discontinuous reinforcement. The algorithm for creating a representative volume element (RVE) must consider random distribution and size of reinforcing particles (RP), prevention of RP interpenetration, and maintaining the desired volume fraction of the reinforcing phase (V_p) in the composite microstructure. Assuming fixed RVE dimensions and randomly determined RP size, the actual V_p value needs to be continuously determined. If the assumed (desired) V_p is lower than the current value, additional reinforcement is added to the RVE. As the RP location is random, some particles may extend beyond the RVE limits, affecting V_p calculation. The research aims to determine the RP volume within the RVE boundaries when RP extends outside. The RVE was discretized with N points, and the number of N_i points within the area occupied by RP was determined. The sought value was calculated using the ratio $N_i/N = V_p/VRVE$, where $VRVE$, is the volume of the RVE. Two discretisation methods, systematised (RI) and random (Monte Carlo (MC)), were employed. The study investigated the effects of discretisation type and number N points on calculation accuracy and microstructure generation time for particle-reinforced composites in sphere, cylinder, and ellipsoid shapes. Systematised discretisation yielded higher accuracy/stability, with number N dependent on RP dimensions. The MC method reduced generation time but introduced instability and significant errors.

Key words: particle-reinforced composites, spatial modelling, representative volume element (RVE), control of volume fraction, numerical integration

1. INTRODUCTION

Today, a steady increase in the use of composites can be observed in various sectors of the economy, such as the defence [1], automotive [2–4] and aerospace [5] industries. Composite materials typically have better strength and performance properties compared to homogeneous materials such as ceramics, metals and plastics. This is due to the fact that beneficial properties of both the matrix (e.g. ductility, impact strength) and reinforcements (e.g. high strength, high elastic modulus, wear resistance) are combined in composites [6]. By appropriate selection of the composite components, their proportions and the distribution and geometry of the reinforcement fractions, a material with the desired mechanical, physical and performance properties can be produced [7–10]. Composite design is a complex process that requires the simultaneous use of experimental and numerical studies [11].

Experimental testing plays a key role, enabling direct investigation of the physical [12,13] and mechanical [14,15] properties of composites. A variety of experiments, such as strength tests, fatigue tests, microstructure analysis or thermal and electrical measurements, are carried out and provide important data for the evaluation and validation of numerical models [16,17].

Numerical tests, such as the finite element method (FEM) [18–21] or the boundary element method (BEM) [22,23], allow the virtual simulation of the behaviour of composites. Numerical mod-

els take into account material parameters, geometry and loading conditions to predict and analyse the response of the composite under different operating conditions. They make it possible to optimize the design of the composite, reduce the cost and time associated with experimental testing, and increase the efficiency of the design process.

One of the key steps in FEM/MEB numerical studies is the preparation of a spatial geometrical model of the composite - a composite fragment that is small enough to preserve the characteristic features and properties of the material, while being large enough for numerical analyses and simulations to be performed on it. Furthermore, this fragment should contain the different components of the composite in the right proportions and take into account their distribution and geometry. Such a composite component is called a representative volume element (RVE) [24,25]. It can be assumed that the RVE is a representation of the microstructure of the composite, and by analysing the RVE, the behaviour and macroscopic properties of the whole composite can be predicted.

The algorithm for generating the RVE, which for composites with discontinuous reinforcement usually follows the random sequential adsorption (RSA) scheme [26–28], must take into account a number of key aspects. Among these aspects are the random distribution and size of reinforcing particles (RPs), the elimination of the possibility of RPs interpenetrating each other, and ensuring the desired volume fraction of the reinforcing phase (V_p) in the composite microstructure. In the context of this latter

aspect, assuming constant RVE dimensions and randomly determined RP sizes, it is necessary to continuously determine the current V_p value. If the assumed V_p value is less than the current one, another reinforcement particle is added to the RVE. However, it should be noted that the location of the RP is also randomly determined, which means that a certain part of the newly added reinforcement particles may protrude outside the boundaries of the RVE. In this case, only the part of the particle that is within the RVE area should be taken into account when calculating the current V_p value. If the reinforcement particle has a regular shape, such as a sphere, cylinder, ellipsoid or cuboid, and its position is such that the axis of symmetry is perpendicular to any of the boundary walls of the RVE, or in the case of a sphere it protrudes only beyond one wall of the representative element, appropriate mathematical formulas can be used to calculate the volume of the particle contained in the RVE. However, if the reinforcement particle has a more complex shape or its position is such that it is not possible to determine unambiguously which part of the particle is inside the RVE, other techniques may be necessary.

While the first two aspects of the RVE formation algorithm (elimination of reciprocal interpenetration of particles and their random distribution) are well described in the literature reports [29–32], the methodology for controlling the assumed V_p appears to be insufficiently studied. An interesting proposal, to solve this problem, for composites with a sphere-shaped RP, has been proposed in papers [28,33] - when the sphere is partially placed outside the RVE, an additional reinforcement particle is created, crossing the opposite wall of the RVE in such a way that the part of the additional particle remaining in the RVE is identical to that projecting outside the RVE (for the original sphere). Another method to find the volume of the reinforcement particle that remains within the RVE is numerical integration. The purpose of this paper is to define the various integration procedures and to investigate the effect of the adopted RVE discretisation model on the accuracy of the calculations. Chapter 2 describes the procedures used along with the discretisation models used. Chapter 3, on the other hand, presents the results of a study on the influence of the discretisation method and the integration parameters used, on the accuracy of the results obtained.

2. APPROACH FOR DETERMINING THE DESIRED VOLUME FRACTION OF REINFORCEMENT PHASE IN RVE

2.1. Main principles and block diagram of the RVE generation algorithm for hybrid composites

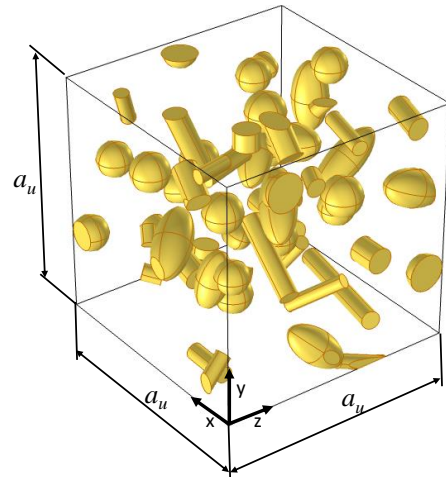
The figure below shows an example of a representative volume element of a hybrid composite (Fig.1a), in which the individual reinforcement particles have the shape of a cylindrical sphere and an ellipsoid. The RVE has the shape of a cube with side a_u . The magnitude of the RVE (side length a_u) is determined by the characteristic dimensions of the RPs and their volume fractions [24,25]. The distribution of the reinforcing particles is random, meaning that the coordinates of the point $P_i(x_i, y_i, z_i)$ ($x_i, y_i, z_i \in [0, a_u]$) are determined randomly (Fig.1b). For cylindrical or ellipsoidal reinforcement particles, the two Euler angles are also determined in the same way: θ_i, ψ_i ($x_i, y_i, z_i \in [0, a_u]$).

Additionally, it is important for the solid objects representing the reinforcement material not to intersect. Therefore, during the generation of subsequent reinforcement elements, the distance

between the axis of the newly formed solid object and the axes of the already existing ones is calculated. The concept of "axis of the solid object" should be understood as follows:

- for a sphere, the axis of the solid object is a line segment of length d_i , with its centre coinciding with the centre of the sphere;
- for a cylinder, the axis of the solid object is a line segment with its ends located at the centres of the bottom and top circular bases;
- for an ellipsoid, the axis of the solid object is a line segment of length l_i , with its centre coinciding with the centre of the ellipsoid.

a)



b)

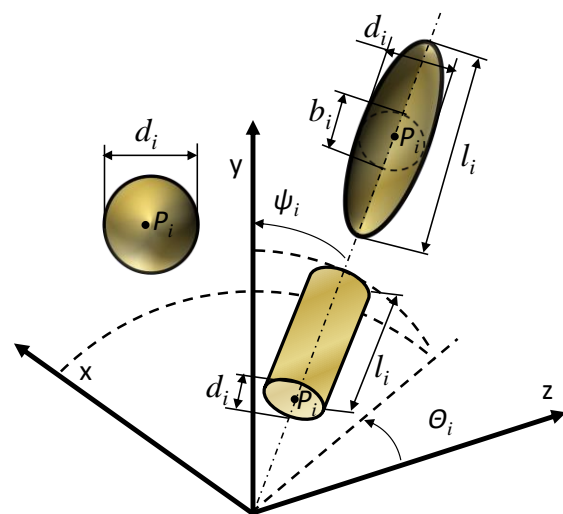


Fig. 1. Representative volume element (a) and single reinforcements in 3D space (b)

This distance must not be less than $1.05 d_{max}$ [26], where d_{max} is the maximum transverse dimension (d_i, b_i , Fig. 1b) of the reinforcement element. The calculation of the distance between RP axes can be carried out as presented in the papers [30,34].

For composites with single reinforcement, algorithms for creating RVEs are discussed in, for example, papers [29,35]. Figure 2 shows a block diagram of the algorithm for creating the RVE of a hybrid composite with the previously described features.

In Figure 2, the operating block, responsible for determining the RP volume remaining within the limits of the RVE when the reinforcement particle extends beyond the representative element, is shown in grey.

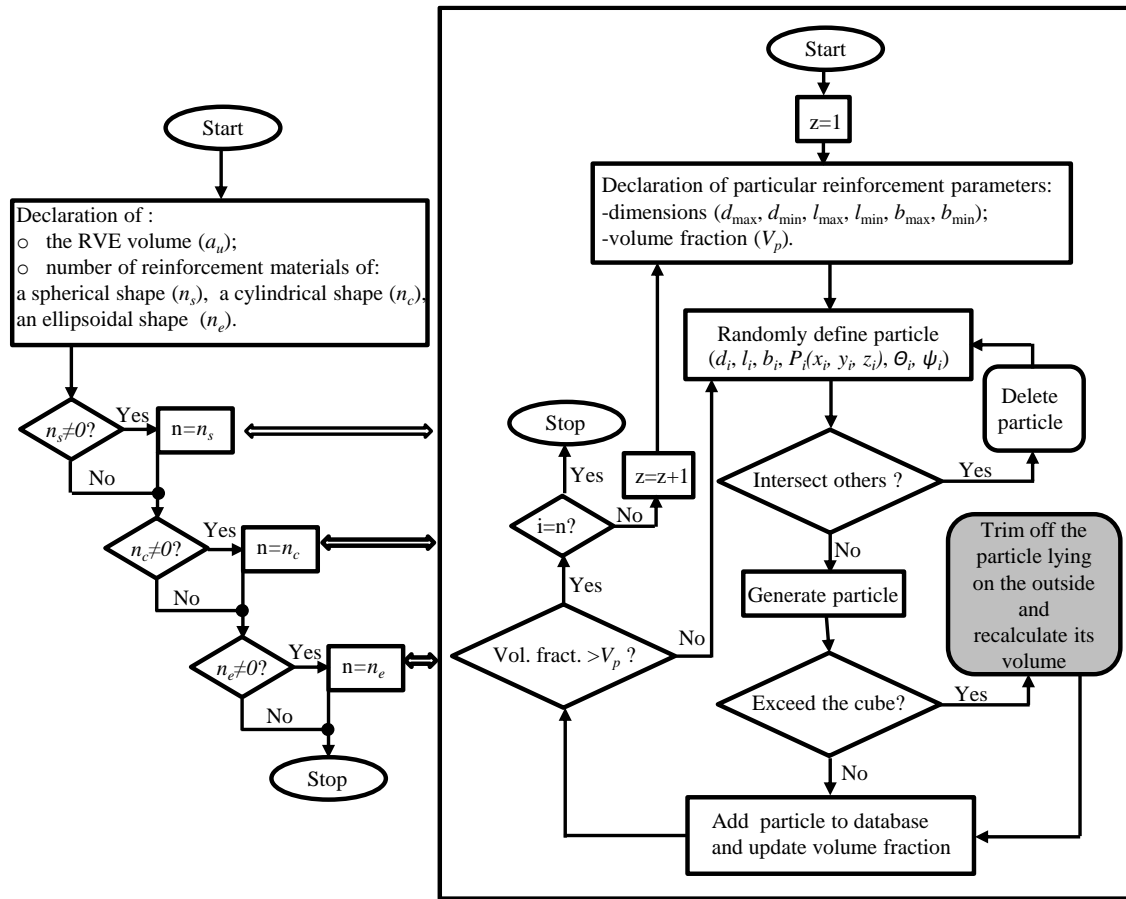


Fig. 2. Block diagram of the algorithm for generating RVE of hybrid composites

The development of operating procedures for this block is the main topic addressed in this paper. The detailed development and description of the processes/procedures involved in its operation are described below.

2.2. Numerical integration methods for estimating the volume fraction of the reinforcement phase in RVE: Integration on a regular grid and Monte Carlo method

Numerical integration is a widely used method in the field of scientific materials research and engineering. It is an efficient method for the estimation of various parameters, such as volume, surface area or inertia, which are important for the characterisation and analysis of different structures. In the context of composite materials analysis, an important aspect is the estimation of the volume fraction of the reinforcement phase in a representative volume element. For this purpose, various numerical integration methods are used to calculate the volume of reinforcement particles within the RVE limits. In this chapter, two popular methods of numerical integration are presented, namely the Monte Carlo (MC) method and integration on a regular/systematised grid (RI). Both of these methods are important in the process of generating the RVE when the reinforcing particles, due to a random distribution, project outside the boundaries of the representative element. With these methods, it is possible to estimate the volume of the portion of the newly generated reinforcement particle that is within the boundaries of the RVE. In general, the procedures for determining the volume of the part of the reinforcement particle remain-

ing in the RVE (nV_p), by means of the two numerical integration methods used, can be divided into four stages: initialisation, discretisation (point or grid generation), point evaluation and calculation of the nV_p volume. A detailed description of each stage is provided below.

2.2.1. Stages in numerical integration

2.2.1.1. Initialisation

At the beginning of the numerical integration process, it is necessary to establish the parameters needed for the calculation, such as the number of points (MC) or the size of the subdivision grid (RI). Using a larger number of points and a smaller grid size results in increased estimation accuracy while increasing the computational load (increased computation time, increased hardware requirements). In practice, the optimal values for the number of points and grid size will depend on the specific research problem, e.g. the shape and dimensions of the RP. There is no single universal value that is suitable for all cases. It is therefore necessary to experimentally adjust and test different values to find the optimal compromise between estimation accuracy, computational load and execution time.

The Monte Carlo method is based on generating random points inside the study area to estimate various parameters. With this method, it is important to choose the number of points appropriately and to maintain randomness in the generation process.

The number of points is important for the accuracy of the es-

timation. The higher the number of points, the more accurate the results obtained. However, it is important to remember that a larger number of points requires more computational time. Therefore, it is important to find an optimal compromise in order to obtain satisfactory estimation accuracy while taking into account the available computational resources. In the paper presented here, the number of points (MC method) and the grid interval (RI method) depended on the overall dimensions of the RVE and RP and were calculated from equations (1) and (2), respectively.

$$N_{MC} = 5 \cdot 10^4 \cdot n \cdot \frac{\min(d_i, b_i, l_i)}{a_u}, n = 1, 2, 3 \dots \quad (1)$$

$$\Delta = (2.5 \cdot n)^{-1} \frac{\min(d_i, b_i, l_i)^2}{a_u}, n = 1, 2, 3 \dots \quad (2)$$

The formulas (1) and (2) have been adopted based on conducted research in such a way that for $n=1$, errors do not exceed 10%.

Knowing the overall dimension of the RVE and the grid interval, the number of grid points can be determined:

$$N_{RI} = \left(\frac{a_u}{\Delta} + 1\right)^3. \quad (3)$$

2.2.1.2. Discretisation

With the Monte Carlo method, points are generated within the study area to represent a sample from space. In this method, it is important to preserve randomness in the process of generating these points. For this purpose, a pseudorandom number generator, available in Java, was used, with which values in the interval $[0,1)$ were generated and multiplied by a_u to obtain random x , y and z coordinates. To exclude duplicates, newly generated points were compared with existing points. If a duplicate point was found, the coordinates of the additional point were drawn, as described above.

In the method of integration on a regular grid, the study area is divided into a regular grid of points. When subdividing, the principle applied was to keep the distribution of points homogeneous - the distance between neighbouring points was identical.

2.2.1.3. Point evaluation

Once each point has been generated, an evaluation is carried out to determine whether it is within the study area. An example of the RVE discretisation for the RI and MC methods is shown in Figure 3a and 3b respectively.

It was assumed that a point M_n is considered to be inside the reinforcement particle if the following conditions are met: sphere-shaped RP:

$$|\overrightarrow{P_i M_n}| \leq d_i/2, \quad (4)$$

cylinder-shaped RP:

$$\begin{cases} x'^2_M + y'^2_M \leq \left(\frac{d_i}{2}\right)^2 \\ 0 \leq z'_M \leq l_i \end{cases}, \quad (5)$$

ellipsoid-shaped RP:

$$\frac{x'^2_M}{(d_i/2)^2} + \frac{y'^2_M}{(b_i/2)^2} + \frac{z'^2_M}{(l_i/2)^2} \leq 1, \quad (6)$$

where: d_i , b_i , l_i - dimensions of the particles of the reinforcement

fraction (Fig. 1b), x'_M, y'_M, z'_M -coordinates of the sampling points in the local reference system, the origin of which is located at point P_i (Fig. 3).

The transformation of the coordinates of the M_n points from the global system (O, x, y, z) to the local system (P_i, x', y', z') was performed based on the following formulae:

$$\begin{bmatrix} x'_M \\ y'_M \\ z'_M \end{bmatrix} = A_1^{3 \times 3} \times A_2^{3 \times 3} \times \begin{bmatrix} x_M - x_P \\ y_M - y_P \\ z_M - z_P \end{bmatrix}, \quad (7)$$

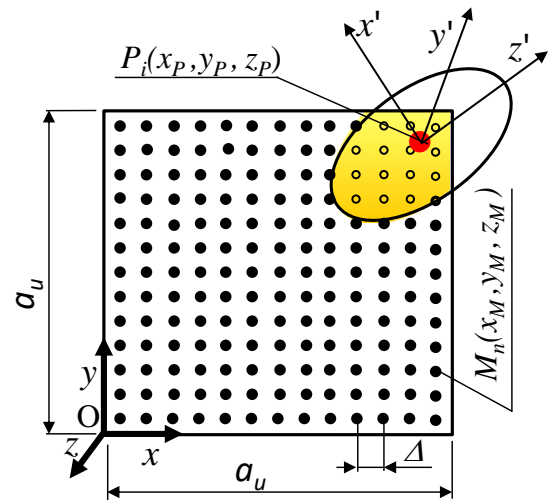
where: x_P, y_P, z_P - coordinates of point P_i (base point RP, Fig. 1b) in the global reference system, $A_1^{3 \times 3}, A_2^{3 \times 3}$ -matrices of rotation by given Euler angles (Fig. 1b).

The matrices are defined by the following formulas:

$$A_1^{3 \times 3} = \begin{bmatrix} 1 & 0 & 0 \\ 0 & \cos(\psi) & -\sin(\psi) \\ 0 & \sin(\psi) & \cos(\psi) \end{bmatrix}, \quad (8)$$

$$A_2^{3 \times 3} = \begin{bmatrix} \cos(\theta) & 0 & \sin(\theta) \\ 0 & 1 & 0 \\ -\sin(\theta) & 0 & \cos(\theta) \end{bmatrix}. \quad (9)$$

a)



b)

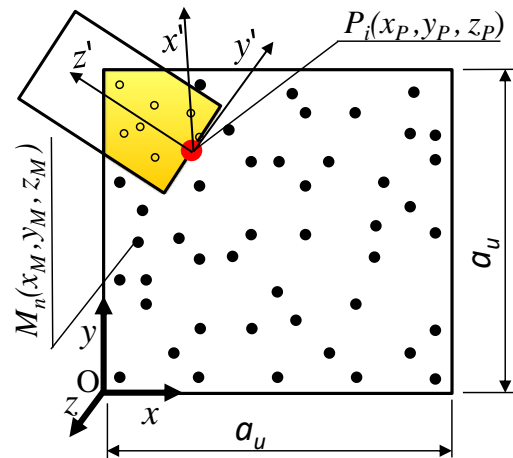


Fig. 3. Sampling in the regular grid integration method (a) and the Monte-Carlo method (b), •-points outside the area of the reinforcement particle, °-points lying inside the reinforcement particle.

The number N_i of points located in the area of the reinforcement particle is determined by summing the points satisfying the conditions described by formulae (4)-(6).

2.2.1.4. Calculation of the nV_p volume

On the basis of the number of N_i points accepted as being inside the study area and the corresponding calculations, it is possible to calculate the estimated volume of the reinforcement phase in a representative volume element (shaded area in Figure 3).

In the RI method, the process involves adding up the volume of all accepted points. A key assumption of this method is that the points are evenly distributed across the study area (Figure 3a). Therefore, the volume of the study area is assumed to be evenly distributed over all grid points. Thus, the volume attributed to one point can be calculated by dividing the total volume of the RVE (a_u^3) by the number of points in the grid (3). In practice, if the grid is dense enough, an accurate approximation of the actual volume can be obtained with this approach. However, for sparser grids, the approximation may be less precise and the result may have a significant error.

For the Monte Carlo method, the volume can be calculated from the ratio of the number of points inside the reinforcement area to the total number of points generated and the volume of the study area (1). In other words, the ratio of the number of points accepted as being within the reinforcement area to the total number of points generated in the study area is calculated. This ratio is then multiplied by the volume of the study area (a_u^3). To increase the accuracy of the results of this method, it is advisable to carry out multiple simulations for the same RVE case. This process involves repeating the point generation and volume estimation and then averaging the results. The repetition of simulations minimises the influence of random factors and results in more precise results.

The volume of the solid remaining in the RVE was therefore determined using the following formula:

$$nV_p = \frac{N_i}{N} a_u^3, \quad (10)$$

where: nV_p - the volume of the solid remaining in the RVE, N - the total number of points used in the sampling ($N = N_{MC}$ or $N = N_{MC}$ calculated for the MC and RI methods from equations (1) and (3) respectively), N_i - the number of points lying inside the reinforcement particle.

3. RESULTS AND DISCUSSION

This section of the paper presents the results of the proposed analyses on the use of integration methods (MC and RI) to determine the volume of the reinforcement phase in the RVE. The results obtained are discussed along with their interpretation and analysis. When modelling real composites, the location and dimensions of the reinforcement particles are determined randomly, as this reflects the inherent complexity and heterogeneity of real composite materials. However, in this presented study, it was decided to generate an RVE with a single reinforcing particle whose dimensions and location were identical for all simulations. The main advantage of this approach is that the results can be made comparable. Establishing a single reinforcing particle with the same parameters for all simulations makes it possible to compare results without the influence of randomness on the results. This makes it possible to accurately assess the effect of different analysis methods (Monte Carlo, RI) on the results for the same particle and to investigate the influence of parameters of these methods, such as the number of sampling points or the number of repetitions in the Monte Carlo method. A RVE with cylindrical, spherical and ellipsoidal particles was modelled, using COMSOL Multiphysics software. The dimensions and location were chosen so that the particle protruded outside the RVE (Figure 5). The following characteristic dimensions of the RVE and reinforcing particles were assumed (Figure 1): $a_u = 50 \mu\text{m}$, $d = 0.2a_u$, $b = 0.25a_u$, $l = a_u$. For each particle, the reference volume V_p of the particles remaining in the RVE was determined using COMSOL's built-in measurement tools.

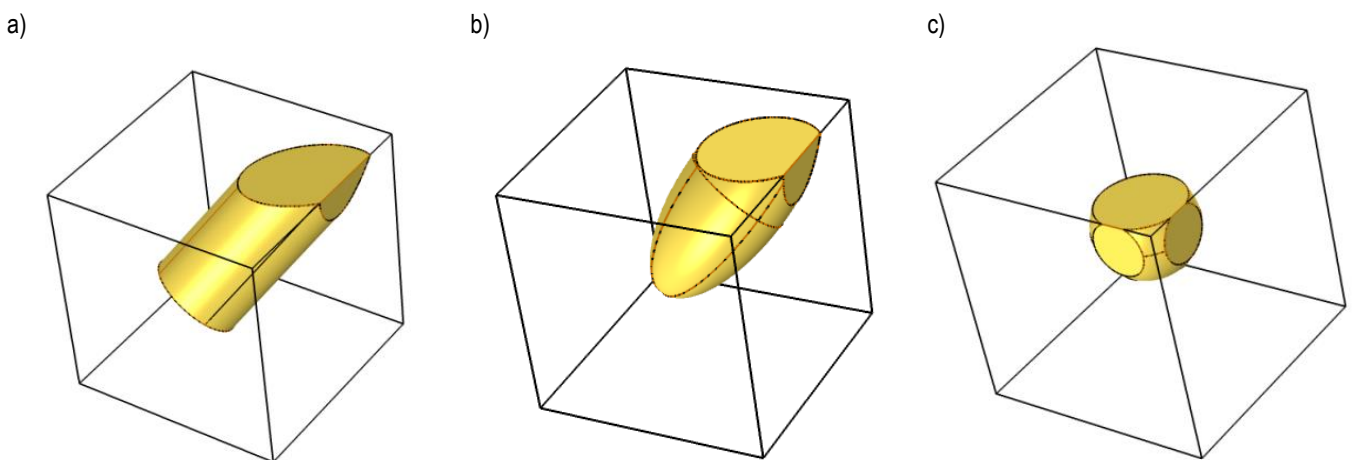


Fig. 4. Modelled RVEs with a reinforcing particle in the shape of a cylinder (a), an ellipsoid (b) and a sphere (c)

The volume V_p was compared with the results obtained by numerical integration using MC and RI methods and the relative error (11) was determined:

$$\Delta_R = \left| \frac{nV_p - V_p}{V_p} \right| \cdot 100\%, \quad (11)$$

where: V_p - the reference volume determined using COMSOL's built-in measurement tools, nV_p - the volume of the reinforcing particle determined using MC and RI (10).

In addition to determining the volume of the particle remaining in the RVE, the calculation time, expressed by the dimensionless parameter t_R , was also determined:

$$t_R = \frac{nt_p}{t_p}, \tag{12}$$

where: nt_p - time to generate the RVE microstructure (Fig.4) with the MC and RI integration procedures active, t_p - time to generate the RVE microstructure (Fig.4) with the MC and RI integration procedures deactivated.

The results of the study of the effect of the method and its parameters on Δ_R and t_R parameters are presented below.

3.1. Analysis of the effect of discretisation density and number of simulation repetitions on the accuracy of the determination of the volume of the reinforcement particle remaining in the RVE and the calculation time

3.1.1. RI method

The effect of the discretisation density, expressed by the multiplicative constant n used in formula (2) to determine the grid interval, on the value of the dimensionless parameters Δ_R and t_R was investigated.

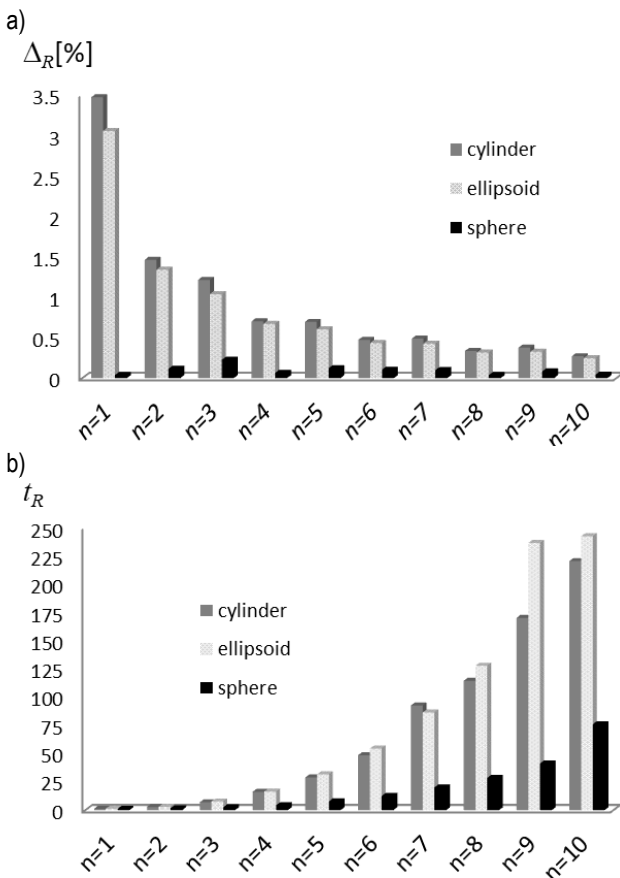


Fig. 5. Effect of discretisation density on calculation time (b) and accuracy (a)

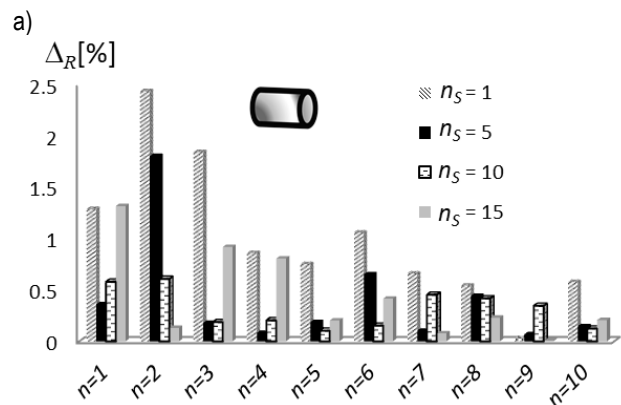
The results obtained are presented in Figure 5. For cylindrical and ellipsoid-shaped reinforcing particles, the calculation accuracy increased with the number of points used for discretisation. For sphere-shaped particles, it was observed that an increase in mesh density could cause a decrease or increase in calculation accuracy. This may be due to the fact that when the grid density is high and the area analysed is relatively small, an edge effect can occur. This is based on the fact that points generated at the edges of spherical particles have a higher probability of being outside the study area. This means that the estimation of the particle volume may be inaccurate, as some points on the edges may be misclassified as outside the area. For cylindrical and ellipsoidal particles, which have a smaller surface-to-volume ratio, the edge effect has less impact on the accuracy of the estimation. The smallest errors were recorded for spherical-shaped particles, while the largest errors were recorded for cylindrical-shaped particles. Differences in calculation accuracy may also be due to the aspect ratio of the solids (ratio of length, width and height) representing the reinforcement. If the solid has a more similar aspect ratio to the interval of the grid of points, the distribution of points will be more uniform, improving the accuracy of the volume estimation. For spherical particles, where the aspect ratio in the three directions is the same, as is the grid interval, the smallest errors were observed.

As for the calculation time, as was to be expected, it always increases with an increase in the number of grid points. The calculation time depended on the shape of the reinforcement particle and was longest for ellipsoid-shaped particles (the condition whose fulfilment causes a point to be considered as being inside the reinforcement particle is the most complex).

Analysing the results shown in Figure 5, it can be seen that there is a compromise between calculation time and accuracy of results, which can be achieved when using, in formula (1), values of n contained in the range $5 \leq n \leq 7$.

3.1.2. MC method

The effect of the number of sampling points, expressed by the multiplicative constant n used in formula (1), and the number of simulation repetitions n_s on the value of the dimensionless parameters Δ_R (Fig.6) and t_R (Fig.7) was investigated. In determining the error in Δ_R , for $n_s \neq 1$, in formula (11) nV_p is the arithmetic mean of the volume of the particle remaining in the RVE determined in all simulations.



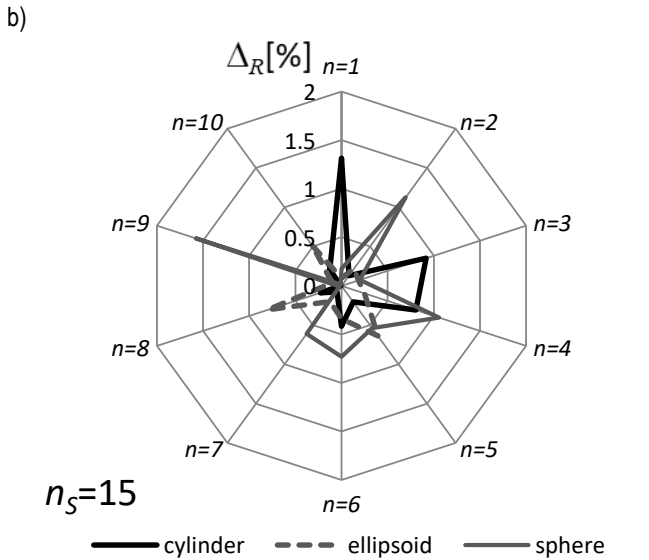


Fig. 6. Influence of the number of sampling points used in the MC method on the calculation accuracy: results for a cylinder-shaped particle when using different numbers of simulation repetitions n_s (a), results obtained for particles of different shapes when using the same number of repetitions $n_s = 15$ (b)

Analysing the results shown in Figure 6, one can conclude that they are characterised by significant randomness, but in most cases a higher number of sampling points and simulation repetitions leads to results with smaller errors. The sensitivity of the method to the shape of the reinforcing particle cannot be clearly determined, as for different numbers of sampling points sometimes more accurate results are obtained for a given particle shape than for others. In most cases, the smallest errors were recorded for sphere-shaped particles. This may be due to their greatest symmetry. Because of this symmetry, the points generated randomly inside a spherical particle are most evenly distributed. This even distribution of sampling points contributes to more accurate analysis results. For particles with other shapes, such as cylinders or ellipsoids, the asymmetry affects a less uniform distribution of sampling points, which can lead to larger errors in the results.

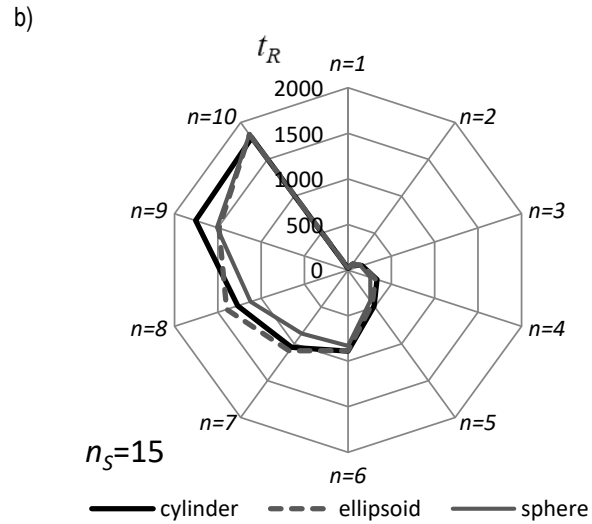
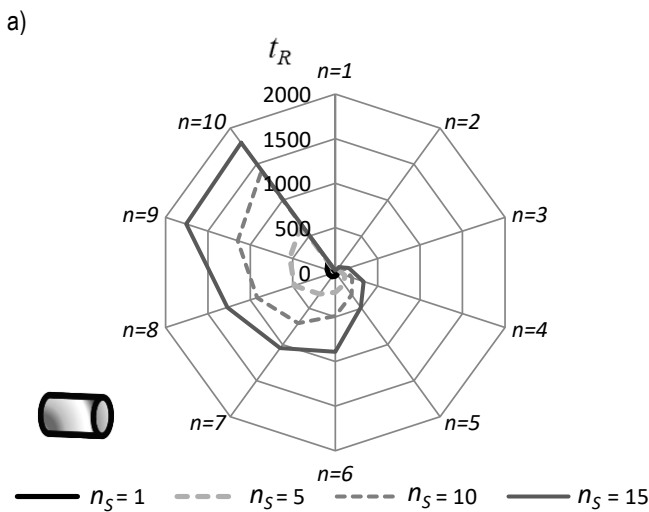


Fig. 7. Influence of the number of sampling points used in the MC method on the calculation time: results for a cylinder-shaped particle when using different numbers of simulation repetitions n_s (a), results obtained for particles of different shapes when using the same number of repetitions $n_s = 15$ (b)

As far as calculation time was concerned, as expected, it increased as the number of sampling points and the number of repetitions increased. The shape of the reinforcing particle also had a slight effect on the calculation time. It was longer for particles for which the condition for verifying that a point belonged to a particle was more complicated - the smallest calculation time occurred for spherical particles and the largest for elliptical particles. The observed deviations from this rule (for example, for $n=9$ the calculation time for a cylindrical particle was longer than for an elliptical particle) may be due to the fact that when drawing n points, repeated points are rejected. If such points occur, the calculation time increases.

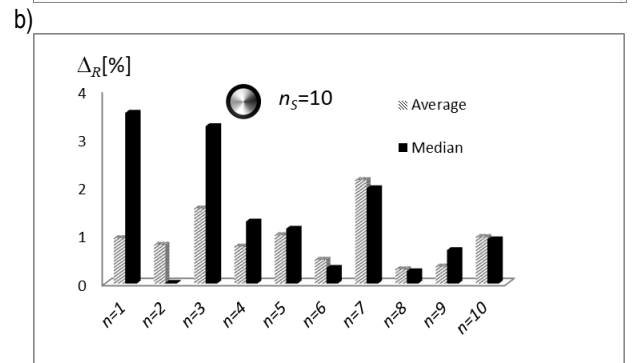
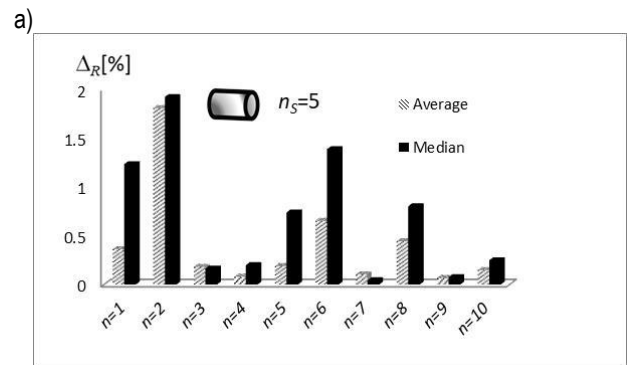


Fig. 8. Influence of the chosen method for nVp determination (arithmetic mean vs median) on the accuracy of the results obtained for cylindrical (a) and spherical (b) shaped particles

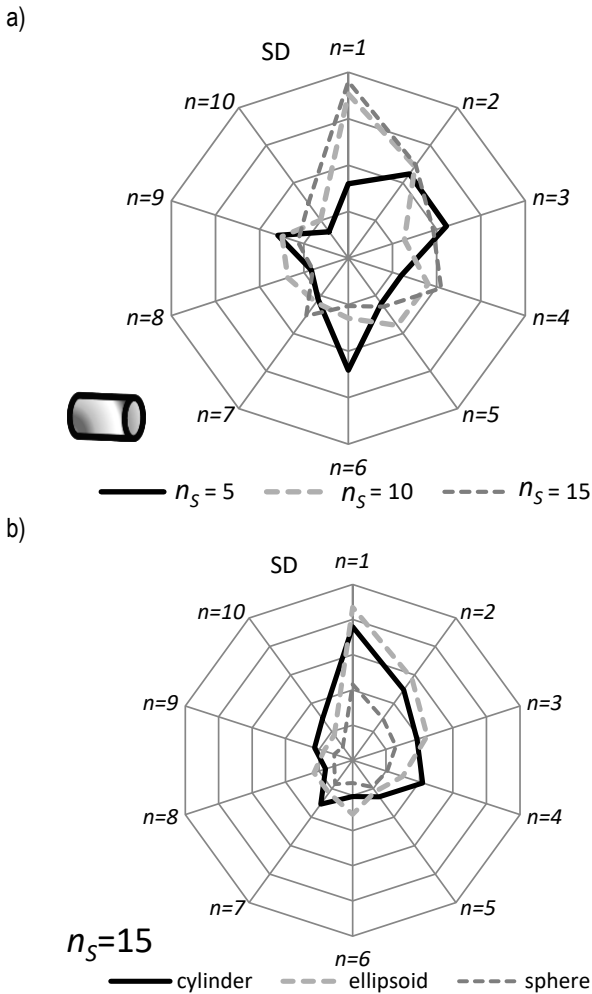


Fig. 9. Influence of the number of sampling points and the number of replicates (a) and the shape of reinforcing particles on the distribution of standard deviation (b)

As mentioned earlier, for simulations with $n_s \neq 1$, nV_p was treated as the arithmetic mean of the volume of particle remaining in the RVE, calculated from all n_s of the simulation. Alternatively, nV_p can also be treated as the median of the results obtained over all iterations. A comparison of the effect of the method of determining the nV_p (arithmetic mean vs. median) on the accuracy of the results is shown in Figure 8. It is noted that, for most of the cases analysed, determining the particle volume using the arithmetic mean led to a higher accuracy of the calculations. There was no significant difference in the computation time of nV_p when using the arithmetic mean and the median.

The paper also analysed the distribution of the standard deviation (SD) and found it to be random (Fig.9). It was observed that a higher number of sampling and simulation repetitions usually results in a lower standard deviation. This effect is due to the fact that a larger number of samples leads to a more representative sample, which in turn translates into more stable and precise results. Increasing the number of simulation repetitions allows better averaging of the results and reduces errors due to random factors. The smallest scatter is observed for spherical particles, as their symmetry contributes to a more uniform distribution of random sampling points. Other particle shapes may have greater variability in results due to less symmetry.

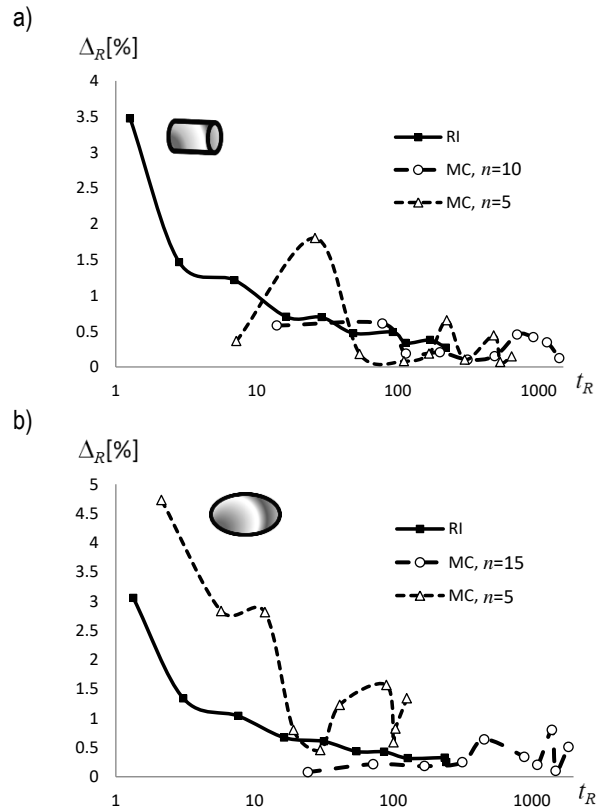
3.2. Comparison of accuracy of results and calculation times obtained using different methods of numerical integration

Figure 10 shows the relative calculation error and duration for the RI and MC methods. By analysing the results obtained, it can be seen that the RI method has a higher stability of results compared to the MC method. Both methods allow similar accuracy to be achieved with similar calculation times. However, in the case of the MC method, it was noted that for some cases e.g. (e.g. ellipsoid-shaped particle, Fig. 9.b, $n=15$) it is possible to achieve better accuracy in less time. However, it is worth noting that the results from the MC method are more unstable and subject to greater fluctuations, which often leads to a larger error with longer calculation times. At a desired error rate of, say, 0.5%, it is well-founded to use the RI method, which provides adequate calculation precision. However, when accepting a higher possible inaccuracy, e.g. of the order of 1.5%, it is worth considering the MC method, as in this case the calculation time is shorter, which can be important for certain applications.

It is worth noting that the RI Method performs particularly well for spherical particles, where accurate results are obtained with short calculation times.

When comparing the two methods, it is important to consider both the accuracy of the calculations and the complexity of the implementation. In terms of these issues, the RI method performs slightly better.

The first aspect to consider is the availability of tools and libraries, as well as the ease of integration into existing software. With the Java programming language integrated into the Comsol environment, the RI method is more favourable to implement. The programme code for the RI method is shorter and does not require as many variables to be defined as for the MC method. This means that, in terms of programming resource availability, the RI method can be more efficient and require less effort.



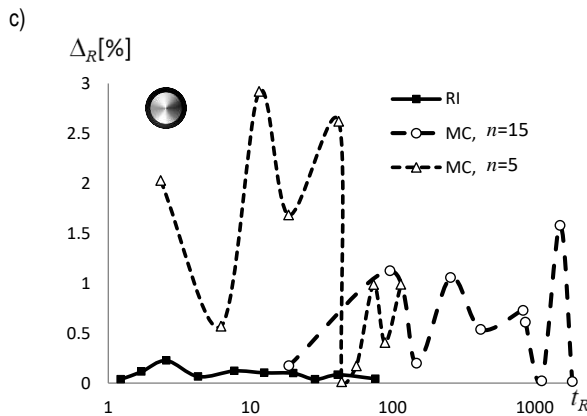


Fig. 10. Relationship between the calculation error and its time for the RI and MC methods for a cylindrical (a), ellipsoid (b) and spherical (c) particle

4. SUMMARY AND CONCLUSIONS

The paper discusses numerical integration procedures employed in analysing the volume of reinforcement particles in algorithms for generating representative volume elements (RVEs) in composites with discontinuous reinforcement, when the reinforcing particles partially extend beyond the RVE. Two methods were compared, where the discretisation was performed in a systematised (RI) or random (MC) manner, focusing on the influence of the integration parameters on the accuracy of calculations and the generation time of the composite microstructure. For the Monte Carlo method, an analysis was conducted on the impact of two parameters: the number of sampling points and the number of simulation repetitions. In the RI method, the focus was solely on the number of sampling points as a parameter. The value of this parameter, for both methods, was related to the size of the reinforcing particles and the dimensional size of the RVE. The study examined how both parameters affect the analysis results and identified their optimal values to achieve precise results with a short microstructure generation time for composites with cylindrical, ellipsoidal, and spherical reinforcing particles.

Both the number of sampling points and the number of simulation repetitions were found to have a significant impact on the accuracy and stability of the results. Increasing the number of sampling points contributed to more precise results, but at the same time increased the RVE generation time. Increasing the number of simulation repetitions in the MC method led to similar effects. In addition, the RI method was observed to have a high stability of results in contrast to the MC method, where significant fluctuation and randomness of the results was noted. Therefore, when an error rate of less than 0.5% is required, the RI method is recommended, as it provides adequate precision in the calculations. On the other hand, when a slightly higher error level, for example 1.5%, is acceptable, the MC method can be considered, which has a shorter calculation time, which can be important in certain applications.

As regards the sensitivity of the tested methods to the shape of the reinforcing particles, in general, the best accuracy of the results was obtained for particles with a spherical shape, which is characterised by the greatest symmetry. Moreover, the calculation time for spherical particles was usually the shortest, while for ellipsoidal particles it was the longest due to the greater complexi-

ty of the condition for checking the belongingness of the sampling point to the particle.

The findings presented here can help designers make decisions regarding the choice of an appropriate discretisation method and number of points when generating models of composites with discontinuous reinforcement. Through optimally selected parameters, designers will be able to achieve accurate analysis results while minimising model generation time, which is of great importance in engineering practice. Further research is planned to focus on developing advanced discretisation algorithms that take into account more complex forms of reinforcement particles.

Nomenclature:

- a_u – side length of a representative volume element (RVE)
- d_i, b_i, l_i – characteristic dimensions of the particles of the reinforcement fraction
- nV_p – the estimated volume of the part of the reinforcement particle remaining in the RVE
- N_{MC} – the number of points used in Monte Carlo method (MC)
- N_{RI} – the number of points used in Regular Integration method (RI)
- Δ – the grid interval used in RI method
- V_p – the reference volume
- Δ_R – the relative error
- t_R – the relative calculation time
- n – the multiplicative constant
- n_s – numbers of simulation repetitions used in MC method

REFERENCES


1. Robinson M. J., Kosmatka J. B. Development of a Short-Span Fiber-Reinforced Composite Bridge for Emergency Response and Military Applications. *Journal of Bridge Engineering* [Internet]. 2008;13(4):388–97. Available from: [https://ascelibrary.org/doi/abs/10.1061/\(ASCE\)1084-0702\(2008\)13:4\(388\)](https://ascelibrary.org/doi/abs/10.1061/(ASCE)1084-0702(2008)13:4(388))
2. Macke A, Schultz B, Rohatgi PK. Metal Matrix Composites Offer the Automotive Industry an Opportunity to Reduce Vehicle Weight, Improve Performance. *Advanced Materials and Processes*. 2012;170:19–23.
3. Mieczkowski G, Szpica D, Borawski A, Diliunas S, Pilkaite T, Leisis V. Application of Smart Materials in the Actuation System of a Gas Injector. *Materials*. Basel Switzerland [Internet]. 2021;14(22). Available from: <https://pubmed.ncbi.nlm.nih.gov/34832384/>
4. Borawski A. Impact of Operating Time on Selected Tribological Properties of the Friction Material in the Brake Pads of Passenger Cars. *Materials* 2021;14(4):884 [Internet]. Available from: <https://www.mdpi.com/1996-1944/14/4/884/htm>
5. Beck AJ, Hodzic A, Soutis C, Wilson CW. Influence of Implementation of Composite Materials in Civil Aircraft Industry on reduction of Environmental Pollution and Greenhouse Effect. *IOP Conference Series: Materials Science and Engineering* [Internet]. 2011;26:12015. Available from: <https://doi.org/10.1088%2F1757-899x%2F26%2F1%2F012015>
6. Richerson DW. *Modern Ceramic Engineering: Properties, Processing, and Use in Design*, Third Edition. CRC Press. 2005.
7. Ibrahim IA, Mohamed FA, Lavernia EJ. Particulate reinforced metal matrix composites — a review. *Journal of Materials Science* [Internet]. 1991;26(5):1137–56. Available from: <https://link.springer.com/article/10.1007/BF00544448>
8. Zhao X, Wang J, Chen Q, Jiang H, Chen C, Tu W. Microstructure design and optimization of multilayered piezoelectric composites with wavy architectures. [Internet]. 2023. Available from: <https://www.tandfonline.com/doi/abs/10.1080/15376494.2023.2172234>

9. Mieczkowski G. Static Electromechanical Characteristics of Piezoelectric Converters with various Thickness and Length of Piezoelectric Layers. *Acta Mechanica et Automatica*. 2019;13(1):30–6.
10. Borawski A, Szpica D, Mieczkowski G, Borawska E, Awad MM, Shalaby RM, et al. Theoretical Analysis of the Motorcycle Front Brake Heating Process during High Initial Speed Emergency Braking. *Journal of Applied and Computational Mechanics*. 2020;6(Special Issue):1431–7.
11. Wang C, Ping X, Zhang Y, Xiao Z, Xiao Y. On the three-dimensional singular stress field near the corner front of revolution-shaped inclusions. *Acta Mechanica* [Internet]. 2021;232(12):4867–95. Available from: <https://link.springer.com/article/10.1007/s00707-021-03078-2>
12. Ran Z, Yan Y, Li J, Qi Z, Yang L. Determination of thermal expansion coefficients for unidirectional fiber-reinforced composites. *Chinese Journal of Aeronautics* [Internet]. 2014;27(5):1180–7. Available from: <https://linkinghub.elsevier.com/retrieve/pii/S1000936114000429>
13. Santos JA, Sanches AO, Akasaki JL, Tashima MM, Longo E, Malmonge JA. Influence of PZT insertion on Portland cement curing process and piezoelectric properties of 0–3 cement-based composites by impedance spectroscopy. *Construction and Building Materials*. 2020;238:117675.
14. Oh KH, Han KS. Short-fiber/particle hybrid reinforcement: Effects on fracture toughness and fatigue crack growth of metal matrix composites. *Composites Science and Technology* [Internet]. 2007;67(7):1719–26. Available from: <http://www.sciencedirect.com/science/article/pii/S026635380600251X>
15. Sijo MT, Jayadevan KR. Analysis of Stir Cast Aluminium Silicon Carbide Metal Matrix Composite: A Comprehensive Review. *Procedia Technology* [Internet]. 2016;24:379–85. Available from: <http://www.sciencedirect.com/science/article/pii/S2212017316301360>
16. Caban J, Drozdziel P, Ignaciuk P, Kordos P. The impact of changing the fuel dose on chosen parameters of the diesel engine start-up process. *Transport Problems*. 2019;14(4):51–62.
17. Szpica D. Fuel dosage irregularity of LPG pulse vapor injectors at different stages of wear. *Mechanika*. 2016;22(1):44–50.
18. Duschlbauer D, Böhm HJ, Pettermann HE. Computational Simulation of Composites Reinforced by Planar Random Fibers: Homogenization and Localization by Unit Cell and Mean Field Approaches. [Internet]. 2006;40(24):2217–34. Available from: <https://journals.sagepub.com/doi/10.1177/0021998306062317>
19. Tornabene F, Luo Y. Microstructure-Free Finite Element Modeling for Elasticity Characterization and Design of Fine-Particulate Composites. *Journal of Composites Science* [Internet]. 2022;6(2):35. Available from: <https://www.mdpi.com/2504-477X/6/2/35/htm>
20. Tu ST, Cai WZ, Yin Y, Ling X. Numerical Simulation of Saturation Behavior of Physical Properties in Composites with Randomly Distributed Second-phase. [Internet]. 2005;39(7):617–31. Available from: <https://journals.sagepub.com/doi/10.1177/0021998305047263>
21. Warguła Ł, Wojtkowiak D, Kukla M, Talaśka K. Symmetric Nature of Stress Distribution in the Elastic-Plastic Range of Pinus L. Pine Wood Samples Determined Experimentally and Using the Finite Element Method (FEM). *Symmetry* 2021;13(1):39 [Internet]. Available from: <https://www.mdpi.com/2073-8994/13/1/39/htm>
22. Yao Z, Kong F, Wang H, Wang P. 2D Simulation of composite materials using BEM. *Engineering Analysis with Boundary Elements*. 2004;28(8):927–35.
23. Chen X, Liu Y. Multiple-cell modeling of fiber-reinforced composites with the presence of interphases using the boundary element method. *Computational Materials Science*. 2001;21(1):86–94.
24. Drugan WJ, Willis JR, Drugan WJ, Willis JR. A micromechanics-based nonlocal constitutive equation and estimates of representative volume element size for elastic composites. *JMPSo* [Internet]. 1996;44(4):497–524. Available from: <https://ui.adsabs.harvard.edu/abs/1996JMPSo..44..497D/abstract>
25. Kanit T, Forest S, Galliet I, Mounoury V, Jeulin D. Determination of the size of the representative volume element for random composites: statistical and numerical approach. *International Journal of Solids and Structures*. 2003;40(13–14):3647–79.
26. Widom B. Random Sequential Addition of Hard Spheres to a Volume. *The Journal of Chemical Physics* [Internet]. 1966;44(10):3888–94. Available from: [/aip/jcp/article/44/10/3888/81726/Random-Sequential-Addition-of-Hard-Spheres-to-a](https://aip/jcp/article/44/10/3888/81726/Random-Sequential-Addition-of-Hard-Spheres-to-a)
27. Böhm HJ, Eckschlagner A, Han W. Multi-inclusion unit cell models for metal matrix composites with randomly oriented discontinuous reinforcements. *Computational Materials Science*. 2002;25(1–2):42–53.
28. Kari S, Berger H, Gabbert U. Numerical evaluation of effective material properties of randomly distributed short cylindrical fibre composites. *Computational Materials Science*. 2007;39(1):198–204.
29. Lee WJ, Son JH, Park IM, Oak JJ, Kimura H, Park YH. Analysis of 3D random Al18B4O33 whisker reinforced Mg composite using FEM and random sequential adsorption. *Materials Transactions*. 2010;51(6):1089–93.
30. Bailakanavar M, Liu Y, Fish J, Zheng Y. Automated modeling of random inclusion composites. *Engineering with Computers*. 2012;30(4):609–25.
31. Zhou J, Qi L, Gokhale AM. Generation of Three-Dimensional Microstructure Model for Discontinuously Reinforced Composite by Modified Random Sequential Absorption Method. *Journal of Engineering Materials and Technology, Transactions of the ASME* [Internet]. 2016;138(2). Available from: <https://asmedigitalcollection.asme.org/materialstechnology/article/138/2/021001/384156/Generation-of-Three-Dimensional-Microstructure>
32. Jin BC, Pelegri AA. Three-dimensional numerical simulation of random fiber composites with high aspect ratio and high volume fraction. *Journal of Engineering Materials and Technology* [Internet]. 2011;133(4). Available from: <https://asmedigitalcollection.asme.org/materialstechnology/article/133/4/041014/469603/Three-Dimensional-Numerical-Simulation-of-Random>
33. Qing H. Automatic generation of 2D micromechanical finite element model of silicon-carbide/aluminum metal matrix composites: Effects of the boundary conditions. *Materials & Design*. 2013;44:446–53.
34. Eberly D. Robust Computation of Distance Between Line Segments. *Geometric Tools* [Internet]. 2018;1–14. Available from: <https://www.geometrictools.com/>
35. Mieczkowski G. Determination of effective mechanical properties of particle - Reinforced composite material with use of numerical approach. *Engineering for Rural Development*. 2020;19:571–7.

This research was financed by the Ministry of Science and Higher Education of Poland with allocation to the Faculty of Mechanical Engineering Białystok University of Technology for the WZ/WM-IIM/5/2023 academic project in the mechanical engineering discipline.

Grzegorz Mieczkowski:  <https://orcid.org/0000-0002-8090-1671>

Dariusz Szpica:  <https://orcid.org/0000-0002-7813-8291>

Borawski Andrzej:  <https://orcid.org/0000-0001-5817-655X>



This work is licensed under the Creative Commons BY-NC-ND 4.0 license.